

Probing Biocatalytic Transformations with Luminescent DNA/Silver Nanoclusters

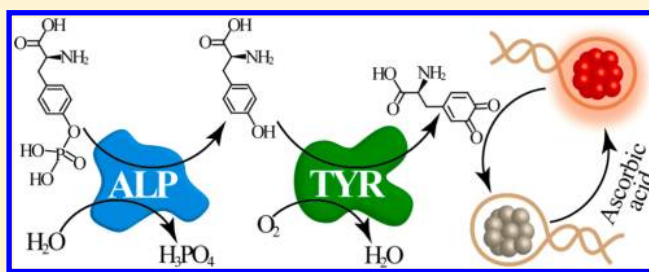
Xiaoqing Liu, Fuan Wang, Angelica Niazov-Elkan, Weiwei Guo, and Itamar Willner*

Institute of Chemistry, Center for Nanoscience and Nanotechnology, The Hebrew University of Jerusalem, Jerusalem 91904, Israel

S Supporting Information

ABSTRACT: DNA-stabilized Ag nanoclusters, AgNCs, act as fluorescent labels for probing enzyme activities and their substrates. The effective quenching of AgNCs by H_2O_2 enables the probing of H_2O_2 -generating oxidases. This is demonstrated by following the glucose oxidase-stimulated oxidation of glucose through the enzyme-catalyzed formation of H_2O_2 . Similarly, the effective quenching of the AgNCs by quinones enabled the detection of tyrosinase through the biocatalyzed oxidation of tyrosine, dopamine, or tyramine to the respective quinone products. The sensitive probing of biocatalytic processes by the AgNCs was further implemented to follow bienzyme catalytic cascades involving alkaline phosphatase/tyrosinase and acetylcholine esterase/choline oxidase. The characterization of the alkaline phosphatase/tyrosinase cascade enabled the ultrasensitive detection of alkaline phosphatase (5×10^{-5} units/mL) and the detection of *o*-phospho-L-tyrosine that is an important intracellular promoter and control growth factor.

KEYWORDS: Ag nanoclusters, fluorescence, enzyme, tyrosinase, alkaline phosphatase, acetylcholine esterase



Metallic nanoparticles, NPs, or semiconductor quantum dots, QDs, find growing interest for probing biocatalytic transformations or proteins and biologically relevant small molecules.¹ For example, the growth of gold nanoparticles (AuNPs) by oxidases,² NAD^+ -dependent enzymes,³ or acetylcholinesterase⁴ was used to probe glucose oxidase, GOx, or alcohol dehydrogenase and their substrates and to follow the inhibition of enzymes. The neurotransmitter-mediated growth of AuNPs was applied for the analysis of the neurotransmitter L-DOPA and the detection of tyrosinase.⁵ Also, Pt nanoparticles modified with a tyrosine methyl ester capping layer were implemented for the electrochemical analysis of tyrosinase through the electrocatalyzed reduction of H_2O_2 .⁶ Alternatively, enzyme- or protein-induced assembly or disassembly of AuNPs was applied for the colorimetric screening of the activities of HRP,⁷ β -lactamase,⁸ phospholipase,⁹ proteases,¹⁰ and alkaline phosphatase¹¹ and the activity and inhibition of endonuclease¹² or kinase.¹³ Also, peptide- or DNA-functionalized nanoparticles for the detection of low-molecular-weight biomolecules, proteins, and enzymatic activity were reported.¹⁴ Similarly, semiconductor QDs have been widely applied in bioanalysis through the luminescence detection of biorecognition events and biocatalytic processes.¹⁵ Different optical assays that involve chemically modified QDs and implementation of fluorescence resonance energy transfer or electron transfer quenching mechanisms were used to follow biocatalytic processes.^{16–22} Also, the biocatalyzed growth or aggregation of QDs was used to follow enzymatic processes.^{23–25} For example, enzymatic transformations were followed by the luminescence properties of QDs, and biocatalytic processes involving polymerase,¹⁶ NAD^+ -dependent enzymes,¹⁷

tyrosinase,¹⁸ protease,¹⁹ telomerase,²² kinase,²³ and glucose oxidase²⁴ were probed by QDs. Also, semiconductor QDs were used for the photoelectrochemical detection of various enzyme substrates such as NADH,²⁶ glucose,²⁷ and acetylcholinesterase inhibitors.²⁸

Recently, the formation of fluorescent metallic nanoclusters (or nanodots), especially the DNA-protected silver nanoclusters (AgNCs/DNA), was reported.²⁹ Bright silver nanoclusters (AgNCs) can be synthesized using guanine- or cytosine-rich DNA as templates, and the AgNCs typically consist of only several atoms. They have interesting features, such as ultrasmall size, tunable emission, high luminescence quantum yields, good photostability and biocompatibility, low toxicity, and good water solubility, turning the nanoclusters as good candidates for biological applications.³⁰ Fluorescent AgNCs have been applied for the detection of metal ions, such as Hg^{2+} and Cu^{2+} ,³¹ thiol-functionalized biomolecules such as cysteine, homocysteine, and glutathione,³² DNA aptamer–substrate complexes such as IgE and thrombin,³³ single nucleotide mutation in DNA,³⁴ and microRNAs (miRNAs).³⁵ The AgNCs/DNA were also used as biolabels for cell imaging.³⁶

Here we wish to report on the novel application of fluorescent AgNCs/DNA for the probing of biocatalytic transformations of different enzyme systems, e.g., glucose oxidase (GOx) and tyrosinase (TYR), and following the biocatalyzed reactions of enzyme cascades, e.g., the alkaline phosphatase/tyrosinase

Received: November 20, 2012

Revised: December 17, 2012

Published: December 19, 2012

(ALP/TYR) cascade and the acetylcholinesterase/choline oxidase (AChE/ChOx) cascade.

The fluorescent DNA-protected silver nanoclusters (AgNCs/DNA) were prepared by the sodium borohydride reduction of silver ions associated with the sequence-specific DNA structure.^{29a} The specific sequence is detailed in the experimental section in the Supporting Information. Previous studies have indicated that the AgNCs consist of fewer than six atoms, exhibiting a hydrodynamic radius of around 3 nm.^{29a,e} The fluorescence of the AgNCs associated with the template DNA is quenched by hydrogen peroxide (H_2O_2) (Figure 1A). The fluorescence

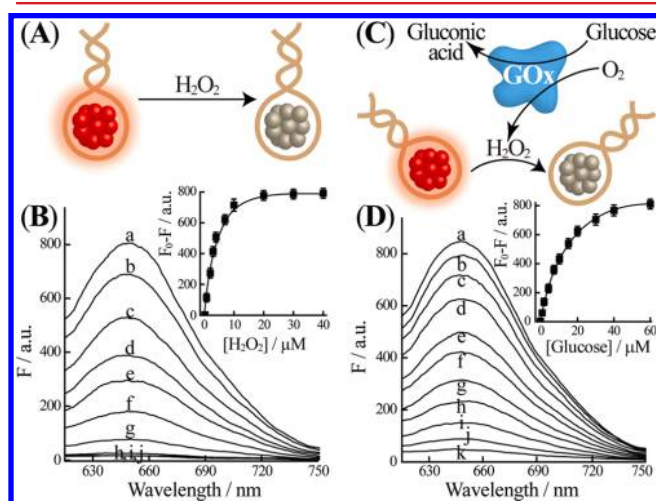


Figure 1. (A) Fluorescence quenching of the AgNCs/DNA by H_2O_2 . (B) Fluorescence spectra of the AgNCs/DNA upon the addition of different concentrations of H_2O_2 : (a) 0, (b) 1, (c) 2, (d) 3, (e) 4, (f) 7, (g) 10, (h) 20, (i) 30, and (j) 40 μM . Inset: calibration curve corresponding to the quenching of the fluorescence of the AgNCs at $\lambda = 648 \text{ nm}$, at different concentrations of H_2O_2 . (C) Fluorescence quenching of the AgNCs/DNA by glucose oxidase (GOx)-catalyzed generation of H_2O_2 . (D) Fluorescence spectra of the AgNCs/DNA upon the glucose oxidase-mediated oxidation of different concentrations of glucose in the presence of 40 nM glucose oxidase: (a) 0, (b) 1, (c) 2, (d) 4, (e) 7, (f) 10, (g) 15, (h) 20, (i) 30, (j) 40, and (k) 60 μM . Inset: the derived calibration curve. Fluorescence spectra were recorded after a fixed time interval of 1.5 h. F_0 corresponds to the fluorescence of the system in the absence of analyte, and F is the fluorescence of the system upon addition of the respective analyte.

spectra of the AgNCs in the presence of variable concentrations of H_2O_2 are shown in Figure 1B. As the concentration of H_2O_2 increases, the quenching process is intensified. The detection limit for analyzing H_2O_2 corresponds to 50 nM. Although the detailed quenching mechanism is not fully understood, the quenching process may involve the oxidation of the surface-bound Ag atoms associated with the nanoclusters to yield oxide surface traps for the excited electrons that prohibit radiative recombination. Similar H_2O_2 quenching of the luminescence of semiconductor QDs (CdSe/ZnS, CdTe) was previously reported,²⁰ and surface oxide traps were spectroscopically identified.³⁷

The quenching of the fluorescence of the AgNCs by H_2O_2 enabled the implementation of the AgNCs/DNA as versatile fluorescence labels for optical detection of the activity of oxidases and their substrates. For example, we used the AgNCs to follow the activity of glucose oxidase, GOx, and to quantitatively detect glucose (Figure 1C). The oxidases catalyze the oxidation of their respective substrates by O_2 to form the

oxidized substrates and H_2O_2 . As the concentration of H_2O_2 in the systems is controlled by the substrates, the resulting fluorescence quenching of the AgNCs provides a quantitative readout signal for the respective substrate. Accordingly, the fluorescent AgNCs/DNA were treated with GOx in the presence of different concentrations of glucose, and the luminescence of the AgNCs was recorded after a fixed time interval of 1.5 h. The selected time interval for analyzing glucose by the system is based on time-dependent fluorescence changes of the AgNCs/DNA in the presence of fixed concentrations of GOx/glucose (see Figure S1, Supporting Information). Figure 1D depicts the fluorescence spectra of the AgNCs resulting from the activation of biocatalyzed oxidation of glucose and the generation of H_2O_2 . As the concentration of glucose increases, the quenching of the fluorescence of the AgNCs is enhanced, consistent with the higher-content generation of H_2O_2 . The derived calibration curve is presented in Figure 1D, inset. The system enabled the detection of glucose with a detection limit corresponding to 150 nM, which is lower than the optical platforms based on GOx-catalyzed biocatalytic growth of Au nanoparticles,² or GOx-mediated growth of fluorescent QDs,²⁴ and electrochemical platforms based on carbon nanomaterials or Au nanoparticles.³⁸ Control experiments revealed that no quenching of the fluorescence of the AgNCs occurred in the absence of GOx and in the presence of glucose/ O_2 or in the presence of GOx and in the absence of glucose/ O_2 (see Figure S2). These results indicate that the quenching of the nanoclusters originates from the GOx/glucose-generated H_2O_2 and that this photophysical process enabled the quantitative assay of glucose.

The AgNCs embedded in the DNA structure were further used to monitor the activity of tyrosinase (TYR). Tyrosinase catalyzes the oxidation of phenol derivatives to *o*-benzoquinone derivatives. Elevated amounts of the enzyme are found in melanoma cancer cells, and it is considered as a useful biomarker for these cancer cells.³⁹ Previous studies have reported on the optical and photoelectrochemical detection of tyrosinase by tyrosine methyl ester-functionalized Pt nanoparticles and semiconductor CdS or CdSe–ZnS QDs.^{6,18} However, these methods require the tedious functionalization and stabilization of the nanoparticles.

We find that *p*-benzoquinone (1) or *o*-naphthoquinone (2), the analogues of the biocatalyzed oxidation product of the tyrosinase substrate, quench the luminescence of the AgNCs (Figure 2A). The quenching of the AgNCs by the quinone derivatives enables the sensitive detection of the quinones, and the detection limits for analyzing 1 or 2 correspond to 400 and 500 pM, respectively (Figure 2B,C). Since there is no spectral overlap between the emission spectrum of the AgNCs and the absorption spectrum of benzoquinone (1) or naphthoquinone (2), an electron transfer quenching mechanism is supported.

The effective quenching of the fluorescence of the AgNCs/DNA hybrid by quinones was then used to assay tyrosinase (Figure 3A). A series of tyrosinase substrates, e.g., tyramine (3), dopamine (4), and tyrosine (5), are applied to follow the activity of tyrosinase. Tyrosinase catalyzes the oxidation of the substrates 3 or 5 to *o*-hydroquinone derivatives, which are further oxidized to *o*-quinone derivatives (6). Accordingly, treatment of dopamine (4) with variable concentrations of tyrosinase under oxygen, for a fixed time interval of 1.5 h, resulted in different quenching efficiencies of the fluorescent AgNCs (Figure 3B). For time-dependent quenching of the AgNCs, see Figure S3. As the concentration of the dopamine (4) increases, the quenching of the fluorescence of the AgNCs is enhanced, consistent with the

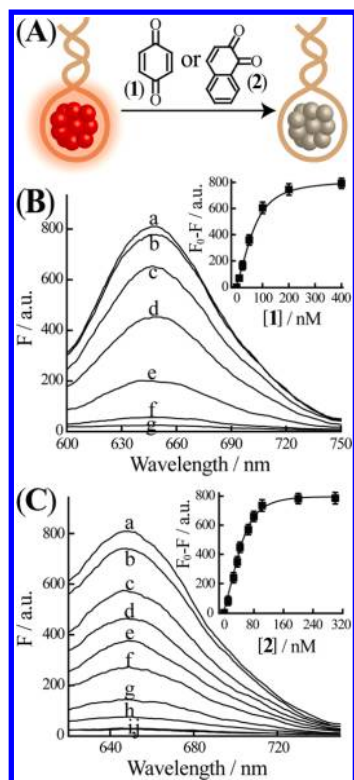


Figure 2. (A) Fluorescence quenching of the AgNCs/DNA by *p*-benzoquinone (1) or *o*-naphthoquinone (2). (B) Fluorescence spectra of the AgNCs/DNA in the presence of different concentrations of *p*-benzoquinone: (a) 0, (b) 5, (c) 25, (d) 50, (e) 100, (f) 200, and (g) 400 nM. Inset: resulting calibration curve. F_0 corresponds to the fluorescence of the system in the absence of quinone derivatives, and F is the fluorescence resulting in the system in the presence of different amounts of quinone derivatives. (C) Fluorescence spectra of AgNCs/DNA in the presence of different concentrations of *o*-naphthoquinone: (a) 0, (b) 10, (c) 25, (d) 35, (e) 40, (f) 65, (g) 80, (h) 100, (i) 200, and (j) 300 nM. Inset: resulting calibration curve.

higher contents of quinone generated by the biocatalytic system. Figure 3B inset shows the calibration curve corresponding to the quantitative analysis of tyrosinase by the fluorescence quenching of the AgNCs/DNA. The method enabled the analysis of tyrosinase with a detection limit corresponding to 5×10^{-5} U (1×10^{-4} U/mL). This sensing platform reveals an impressive detection limit that is ca. 10^4 -fold lower than other nanoparticles-based tyrosinase sensing platforms, such as Pt nanoparticles or QDs.^{6,18} The value is also nearly 2 and 3 orders of magnitude smaller than the detection limit of reported optical and electrochemical platforms, respectively.⁴⁰ Figure 3C shows that addition of ascorbic acid to the tyrosinase/dopamine system regenerates the original fluorescence signal of the AgNCs. This is due to the fact that ascorbic acid reduces dopaquinone to dopamine, thus prohibiting the formation of dopaquinone, which acts as the quencher of the AgNCs. Control experiments revealed that tyrosinase alone or ascorbic acid alone did not affect the fluorescence of the AgNCs (see Figures S4 and S5). Similarly, the AgNCs/DNA fluorescent hybrid has been implemented for the quantitative analysis of the tyrosinase using tyrosine or tyramine as substrates (see Figures S6 and Figure S7).

Important issues that need to be considered upon using AgNCs as optical labels to follow biocatalytic processes relate to the possible effect (inhibition) of AgNCs on the activity of the enzymes and the possible use of the AgNCs as optical labels

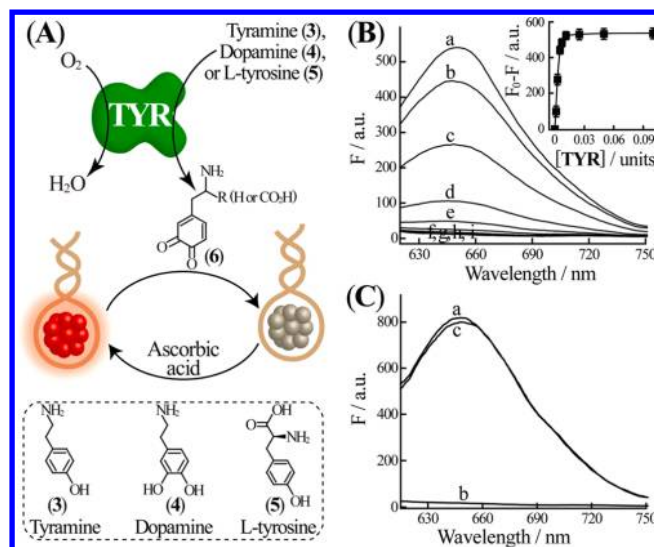


Figure 3. (A) Analysis of tyrosinase (TYR) activity by the quinone-quenched fluorescence of AgNCs/DNA. (B) Fluorescence spectra of the AgNCs/DNA upon analyzing variable concentrations of tyrosinase in the presence of 4 μ M dopamine (4) for a fixed time interval of 1.5 h: (a) 0, (b) 0.001, (c) 0.0025, (d) 0.005, (e) 0.0075, (f) 0.01, (g) 0.025, (h) 0.05, and (i) 0.1 units. Inset: resulting calibration curve. F_0 corresponds to the fluorescence of the system in the absence of tyrosinase, and F is the fluorescence resulting in the system in the presence of different amounts of tyrosinase. (C) Fluorescence spectra corresponding to the AgNCs/DNA (a) in the absence of tyrosinase and dopamine (4), (b) in the presence of 0.025 units tyrosinase and 4 μ M dopamine (4), and (c) fluorescence regeneration of the AgNCs/DNA upon addition of 10 μ M ascorbic acid to the system generated in (b).

in biological fluids. The possible effect of AgNCs on the activity of the enzymes was examined by assaying the activity of glucose oxidase, GOx, in the absence or presence of AgNCs. Figure S8 reveals that the AgNCs do not have any effect on the catalytic activity of GOx. Thus, we conclude that enzymes may resist the environment of AgNCs and retain their activities. Nonetheless, it would be essential for any biosensing applications to specifically examine the effect of AgNCs on the enzymes involved in the process. The use of AgNCs as optical labels for sensing events in biological fluids was addressed by the assaying tyrosinase, TYR, with the AgNCs in diluted plasma samples. Figure S9 describes the experimental results upon assaying of tyrosinase in the plasma sample, using the assay shown in Figure 3A. We find that tyrosinase can be monitored in the diluted plasma using the AgNCs as optical labels.

The successful analysis of glucose oxidase or tyrosinase by the AgNCs/DNA fluorescent hybrid suggests that the AgNCs/DNA system may be implemented to follow other biocatalytic processes and, particularly, enzyme cascades. This is exemplified in Figure 4A with the assay of alkaline phosphatase (ALP) and the quantitative analysis of *o*-phospho-L-tyrosine (7) using a bienzyme cascade consisting of alkaline phosphatase and tyrosinase (Figure 4A). Alkaline phosphatase catalyzes the dephosphorylation of proteins or nucleic acids, and it regulates many cellular pathways. It is an important biomarker in clinical practice, and elevated amounts of alkaline phosphatase relate to bone, liver, and cancer diseases.⁴¹ The analysis of alkaline phosphatase is based on the primary alkaline phosphatase hydrolysis of *o*-phospho-L-tyrosine (7) to L-tyrosine (5). The subsequent tyrosinase (TYR)-catalyzed oxidation of L-tyrosine (5) yields

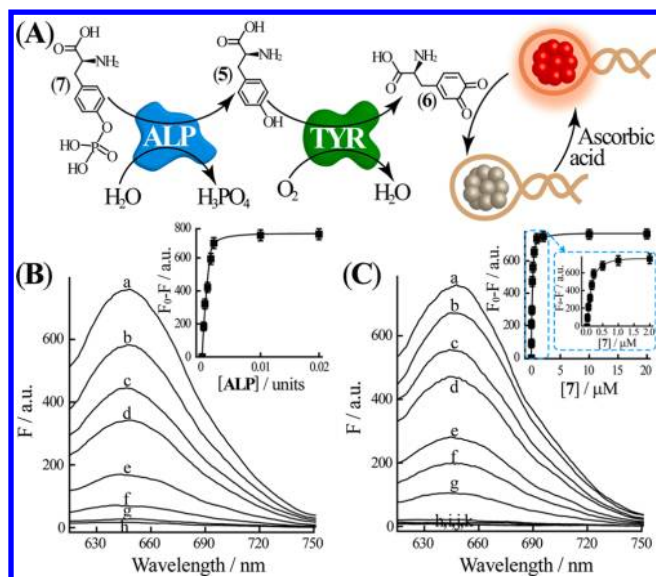


Figure 4. (A) Following the bienzyme cascade tyrosinase/alkaline phosphatase (TYR/ALP) by the AgNCs/DNA fluorescent hybrid. (B) Fluorescence spectra of the AgNCs/DNA upon analyzing different amounts of alkaline phosphatase: (a) 0, (b) 0.00025, (c) 0.0005, (d) 0.001, (e) 0.0015, (f) 0.002, (g) 0.01, and (h) 0.02 units, in the presence of *o*-phospho-L-tyrosine (7), 20 μM, and tyrosinase, 0.2 units. Inset: resulting calibration curve. F_0 corresponds to the fluorescence of the system in the absence of alkaline phosphatase, and F is the fluorescence of the system with different amounts of alkaline phosphatase. (C) Analysis of variable concentrations of *o*-phospho-L-tyrosine (7) by the AgNCs/DNA: (a) 0, (b) 0.01, (c) 0.05, (d) 0.1, (e) 0.15, (f) 0.2, (g) 0.5, (h) 1, (i) 2, (j) 10, and (k) 20 μM, in the presence of tyrosinase, 0.2 units, and alkaline phosphatase, 0.02 units. Inset: resulting calibration curve corresponding to the fluorescence quenching of the AgNCs/DNA at variable concentrations of 7. Fluorescence spectra were recorded after a fixed time interval of 1.5 h.

L-DOPA quinone (6) which quenches the fluorescence of the AgNCs. In this process, the concentrations of the quencher units L-DOPA quinone (6) are controlled by the content of L-tyrosine (5), and the concentrations of L-tyrosine (5) are related to the effectiveness of the hydrolytic cleavage of *o*-phospho-L-tyrosine (7) by alkaline phosphatase. Thus, by retaining the concentrations of all components in the system constant, except the concentration of alkaline phosphatase, and allowing the biocatalytic reactions in the system to proceed for a fixed time interval, the resulting fluorescence quenching of the AgNCs/DNA relates directly to the concentration of alkaline phosphatase. Figure 4B shows the fluorescence responses of the AgNCs upon including different concentrations of alkaline phosphatase in the system and its operation for a fixed time interval of 1.5 h (for time-dependent quenching of the AgNCs, see Figure S10). The calibration curve is shown in Figure 4B inset. Alkaline phosphatase is detected at a sensitivity as low as 2.5×10^{-5} units (5×10^{-5} U/mL), a value that is 4 orders of magnitude more sensitive than other optical methods based on aggregation of silver nanoparticles^{11a} or gold nanoparticles.^{11b}

o-Phospho-L-tyrosine (7) has been reported to inhibit the growth of human renal and breast carcinoma cells, to increase total cellular PTPase activity in MDA-MB 468 breast carcinoma cells and to decrease epidermal growth factor receptor (EGFR) phosphorylation and subsequent activity. *o*-Phospho-L-tyrosine also finds a protective effect on TP53 wild-type cells against ionizing radiation.⁴² Thus, the fluorescent AgNCs/DNA hybrid

was applied for the quantitative detection of *o*-phospho-L-tyrosine (7). Figure 4C depicts the fluorescence spectra of the AgNCs upon analyzing different concentrations of *o*-phospho-L-tyrosine (7). In these experiments the fluorescence of the AgNCs/DNA was monitored upon subjecting fixed amounts of tyrosinase and alkaline phosphatase to variable concentrations of *o*-phospho-L-tyrosine (7). As the concentration of *o*-phospho-L-tyrosine (7) increases, the quenching of the AgNCs is enhanced, consistent with the higher concentration of L-DOPA quinone (6) generated by the biocatalytic system. Control experiments confirm that the biocatalytic process of the enzyme cascade is only activated in the presence of the two enzymes, tyrosinase and alkaline phosphatase.

The successful probing of the alkaline phosphatase/tyrosinase (ALP/TYR) cascade by the AgNCs/DNA fluorescent hybrid suggested that the Ag nanoclusters might also be implemented to follow the activation of biocatalytic cascades that involve H₂O₂-generating oxidase. This is demonstrated by following the acetylcholinesterase/choline oxidase (AChE/ChOx) cascade. AChE catalyzes the hydrolysis of acetylcholine (8) into choline (9). Acetylcholine is involved in neurological disorders, such as schizophrenia, Tourette's syndrome, Huntington's, Parkinson's, and Alzheimer's diseases.⁴³ The resulting choline (9) is oxidized by O₂ in the presence of choline oxidase (ChOx) as biocatalyst to yield betaine aldehyde (10), while producing H₂O₂ that is followed by the quenching of the fluorescence of the AgNCs (Figure 5A). The fluorescence quenching of the AgNCs, upon addition of variable concentrations of acetylcholine, is shown in Figure 5B. For time-dependent quenching of the AgNCs, see Figure S11. In the absence of acetylcholinesterase or choline oxidase, no fluorescence changes were observed upon the addition of acetylcholine (8) (see Figure S12), while a sharp decrease in the fluorescence of AgNCs was observed upon addition of acetylcholine (8) in the presence of acetylcholinesterase and choline oxidase. This indicates that the biocatalytically generated H₂O₂ leads to the effective quenching of the AgNCs. Evidently, the enzyme cascade is only activated in the presence of the two enzymes and the substrate acetylcholine (8).

The present study has introduced fluorescent DNA-stabilized Ag nanoclusters, AgNCs, as optical labels for following biocatalytic transformations. We demonstrated that H₂O₂ quenches the luminescence of the AgNCs, and this enables the probing of biocatalytic oxidase-stimulated H₂O₂-generating biotransformations. This was exemplified with the analysis of the glucose oxidase (GOx)-mediated oxidation of glucose that yields gluconic acid and H₂O₂. Also, quinone derivatives quench the luminescence of the AgNCs, and this function enables the probing of tyrosinase, TYR, a melanoma cancer cell biomarker. The TYR-stimulated oxidation of tyrosine, dopamine, or tyramine yields quinone derivatives that quench the fluorescence of the AgNCs. This enabled the sensitive detection of tyrosinase (detection limit 1×10^{-4} units/mL). The successful analysis of tyrosinase or glucose was further implemented to probe bienzyme biocatalytic cascades. These included the alkaline phosphatase/tyrosinase coupled hydrolysis and oxidation of *o*-phospho-L-tyrosine and the acetylcholine esterase/choline oxidase hydrolysis of acetylcholine and subsequent oxidation of choline. The results pave the way to implement AgNCs as optical labels to follow the activity of other oxidases and other cascaded biocatalytic transformations.

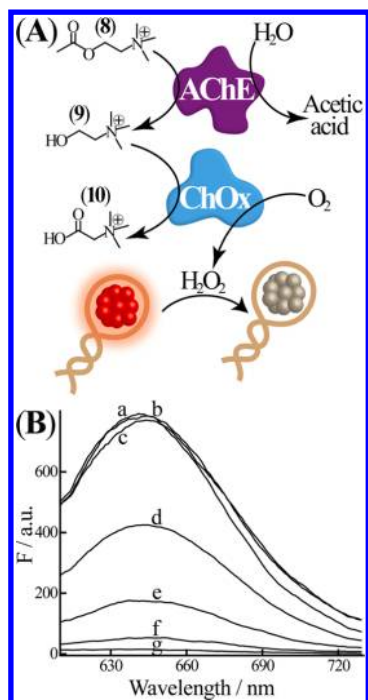


Figure 5. (A) Probing the enzyme cascade acetylcholinesterase/choline oxidase (AChE/ChOx) by the AgNCs/DNA hybrid. (B) Fluorescence spectra of AgNCs/DNA (a) in the absence of acetylcholinesterase, choline oxidase, and acetylcholine (8), (b) in the presence of 500 μ M acetylcholine (8) and in the absence of acetylcholinesterase and choline oxidase, (c) in the presence of 0.2 μ M acetylcholinesterase and 0.4 μ M choline oxidase and in the absence of acetylcholine (8), and (d–g) in the presence of 0.2 μ M acetylcholinesterase, 0.4 μ M choline oxidase, and (d) 25, (e) 100, (f) 200, and (g) 400 μ M acetylcholine (8). Fluorescence spectra were recorded after a fixed time interval of 1.5 h.

■ ASSOCIATED CONTENT

Supporting Information

Experimental section, analysis of tyrosinase activity by AgNCs/DNA using tyrosine or tyramine as substrates, time-dependent quenching of the AgNCs, possible effect of AgNCs on the activity of GOx, tyrosinase analysis in plasma sample, and all the control experiments. This material is available free of charge via the Internet at <http://pubs.acs.org>.

■ AUTHOR INFORMATION

Corresponding Author

*E-mail willnea@vms.huji.ac.il; Tel +972-2-6585272; Fax +972-2-6527715.

Notes

The authors declare no competing financial interest.

■ ACKNOWLEDGMENTS

This study is supported by the Israel Science Foundation, Israel, and by the Volkswagen Foundation, Germany.

■ REFERENCES

(1) (a) Aragay, G.; Pino, F.; Merkoçi, A. *Chem. Rev.* **2012**, *112*, 5317–5338. (b) Willner, I.; Willner, B. *Nano Lett.* **2010**, *10*, 3805–3815. (c) Wang, F.; Liu, X.; Willner, I. *Adv. Mater.* **2012**, DOI: 10.1002/adma.201201772. (d) De, M.; Ghosh, P. S.; Rotello, V. M. *Adv. Mater.* **2008**, *20*, 4225–4241. (e) Rosi, N. L.; Mirkin, C. A. *Chem. Rev.* **2005**, *105*, 1547–1562. (f) Ho, J. A.; Chang, H.-C.; Shih,

N.-Y.; Wu, L.-C.; Chang, Y.-F.; Chen, C.-C.; Chou, C. *Anal. Chem.* **2010**, *82*, 5944–5950. (g) Saha, K.; Agasti, S. S.; Kim, C.; Li, X.; Rotello, V. M. *Chem. Rev.* **2012**, *112*, 2739–2779.

(2) Zayats, M.; Baron, R.; Popov, I.; Willner, I. *Nano Lett.* **2005**, *5*, 21–25.

(3) (a) Zhang, L.; Li, Y.; Li, D.-W.; Jing, C.; Chen, X.; Lv, M.; Huang, Q.; Long, Y.-T.; Willner, I. *Angew. Chem., Int. Ed.* **2011**, *50*, 6789–6792. (b) Xiao, Y.; Pavlov, V.; Levine, S.; Niazov, T.; Markovitch, G.; Willner, I. *Angew. Chem., Int. Ed.* **2004**, *43*, 4519–4522.

(4) (a) Liao, S.; Qiao, Y.; Han, W.; Xie, Z.; Wu, Z.; Shen, G.; Yu, R. *Anal. Chem.* **2012**, *84*, 45–49. (b) Pavlov, V.; Xiao, Y.; Willner, I. *Nano Lett.* **2005**, *5*, 649–653.

(5) Baron, R.; Zayats, M.; Willner, I. *Anal. Chem.* **2005**, *77*, 1566–1571.

(6) Yildiz, H. B.; Freeman, R.; Gill, R.; Willner, I. *Anal. Chem.* **2008**, *80*, 2811–2816.

(7) dela Rica, R.; Fratila, R. M.; Szarpak, A.; Huskens, J.; Velders, A. H. *Angew. Chem., Int. Ed.* **2011**, *50*, S704–S707.

(8) Liu, R.; Liew, R.; Zhou, J.; Xing, B. *Angew. Chem., Int. Ed.* **2007**, *46*, 8799–8803.

(9) Aili, D.; Mager, M.; Roche, D.; Stevens, M. M. *Nano Lett.* **2011**, *11*, 1401–1405.

(10) Guarise, C.; Pasquato, L.; Filippis, V. D.; Scrimin, P. *Proc. Natl. Acad. Sci. U. S. A.* **2006**, *103*, 3978–3982.

(11) (a) Wei, H.; Chen, C.; Han, B.; Wang, E. *Anal. Chem.* **2008**, *80*, 7051–7055. (b) Choi, Y.; Ho, N.-H.; Tung, C.-H. *Angew. Chem., Int. Ed.* **2007**, *46*, 707–709.

(12) Xu, X.; Han, M. S.; Mirkin, C. A. *Angew. Chem., Int. Ed.* **2007**, *46*, 3468–3470.

(13) Wang, Z.; Lévy, R.; Fernig, D. G.; Brust, M. *J. Am. Chem. Soc.* **2006**, *128*, 2214–2215.

(14) (a) Xie, X.; Xu, W.; Liu, X. *Acc. Chem. Res.* **2012**, *45*, 1511–1520. (b) Niemeyer, C. M. *Angew. Chem., Int. Ed.* **2010**, *49*, 1200–1216. (c) Rosi, N. L.; Giljohann, D. A.; Thaxton, C. S.; Lytton-Jean, A. K. R.; Han, M. S.; Mirkin, C. A. *Science* **2006**, *312*, 1027–1030. (d) Aili, D.; Stevens, M. M. *Chem. Soc. Rev.* **2010**, *39*, 3358–3370.

(15) (a) Bruchez, M., Jr.; Moronne, M.; Gin, P.; Weiss, S.; Alivisatos, A. P. *Science* **1998**, *281*, 1038–1041. (b) Medintz, I. L.; Uyeda, H. T.; Goldman, E. R.; Mattoussi, H. *Nat. Mater.* **2005**, *4*, 435–446. (c) Freeman, R.; Willner, B.; Willner, I. *J. Phys. Chem. Lett.* **2011**, *2*, 2667–2677.

(16) Suzuki, M.; Husimi, Y.; Komatsu, H.; Suzuki, K.; Douglas, K. T. *J. Am. Chem. Soc.* **2008**, *130*, 5720–5725.

(17) Freeman, R.; Gill, R.; Shweky, I.; Kotler, M.; Banin, U.; Willner, I. *Angew. Chem., Int. Ed.* **2009**, *48*, 309–313.

(18) Gill, R.; Freeman, R.; Xu, J.-P.; Willner, I.; Winograd, S.; Shweky, I.; Banin, U. *J. Am. Chem. Soc.* **2006**, *128*, 15376–15377.

(19) (a) Shi, L.; Paoli, V. D.; Rosenzweig, N.; Rosenzweig, Z. *J. Am. Chem. Soc.* **2006**, *128*, 10378–10379. (b) Prasuhn, D. E.; Feltz, A.; Blanco-Canosa, J. B.; Susumu, K.; Stewart, M. H.; Mei, B. C.; Yakovlev, A. V.; Loukou, C.; Mallet, J. M.; Oheim, M.; Dawson, P. E.; Medintz, I. L. *ACS Nano* **2010**, *4*, 5487–5497.

(20) (a) Gill, R.; Bahshi, L.; Freeman, R.; Willner, I. *Angew. Chem., Int. Ed.* **2008**, *47*, 1676–1679. (b) Yuan, J.; Gaponik, N.; Eychmüller, A. *Anal. Chem.* **2012**, *84*, S047–S052.

(21) Ghadiali, J. E.; Lowe, S. B.; Stevens, M. M. *Angew. Chem., Int. Ed.* **2011**, *50*, 3417–3420.

(22) Patolsky, F.; Gill, R.; Weizmann, Y.; Mokari, T.; Banin, U.; Willner, I. *J. Am. Chem. Soc.* **2003**, *125*, 13918–13919.

(23) Xu, X.; Liu, X.; Nie, Z.; Pan, Y.; Guo, M.; Yao, S. *Anal. Chem.* **2011**, *83*, 52–59.

(24) Saa, L.; Pavlov, V. *Small* **2012**, *8*, 3449–3455.

(25) Saa, L.; Mato, J. M.; Pavlov, V. *Anal. Chem.* **2012**, *84*, 8961–8965.

(26) Schubert, K.; Khalid, W.; Yue, Z.; Parak, W. J.; Lisdat, F. *Langmuir* **2010**, *26*, 1395–1400.

(27) Tanne, J.; Schäfer, D.; Khalid, W.; Parak, W. J.; Lisdat, F. *Anal. Chem.* **2011**, *83*, 7778–7785.

- (28) Pardo-Yissar, V.; Katz, E.; Wasserman, J.; Willner, I. *J. Am. Chem. Soc.* **2003**, *125*, 622–623.
- (29) (a) Richards, C. I.; Choi, S.; Hsiang, J. C.; Antoku, Y.; Vosch, T.; Bongiorno, A.; Tzeng, Y. L.; Dickson, R. M. *J. Am. Chem. Soc.* **2008**, *130*, 5038–5039. (b) Gwinn, E. G.; O'Neill, P.; Guerrero, A. J.; Bouwmeester, D.; Fyngenson, D. K. *Adv. Mater.* **2008**, *20*, 279–283. (c) Petty, J. T.; Zheng, J.; Hud, N. V.; Dickson, R. M. *J. Am. Chem. Soc.* **2004**, *126*, 5207–5212. (d) Vosch, T.; Antoku, Y.; Hsiang, J. C.; Richards, C. I.; Gonzalez, J. I.; Dickson, R. M. *Proc. Natl. Acad. Sci. U. S. A.* **2007**, *104*, 12616–12621. (e) Ritchie, C. M.; Johnsen, K. R.; Kiser, J. R.; Antoku, Y.; Dickson, R. M.; Petty, J. T. *J. Phys. Chem. C* **2007**, *111*, 175–181.
- (30) (a) Choi, S.; Dickson, R. M.; Yu, J. *Chem. Soc. Rev.* **2012**, *41*, 1867–1891. (b) Latorre, A.; Somoza, A. *ChemBioChem* **2012**, *13*, 951–958. (c) Han, B.; Wang, E. *Anal. Bioanal. Chem.* **2012**, *402*, 129–138. (d) Xu, H.; Suslick, K. S. *Adv. Mater.* **2010**, *22*, 1078–1082.
- (31) (a) Guo, W.; Yuan, J.; Wang, E. *Chem. Commun.* **2009**, 3395–3397. (b) Su, Y.-T.; Lan, G.-Y.; Chen, W.-Y.; Chang, H.-T. *Anal. Chem.* **2010**, *82*, 8566–8572.
- (32) (a) Chen, W.-Y.; Lan, G.-Y.; Chang, H.-T. *Anal. Chem.* **2011**, *83*, 9450–9455. (b) Huang, Z.; Pu, F.; Lin, Y.; Ren, J.; Qu, X. *Chem. Commun.* **2011**, *47*, 3487–3489.
- (33) (a) Li, H.; Qiang, W.; Vuki, M.; Xu, D.; Chen, H.-Y. *Anal. Chem.* **2011**, *83*, 8945–8952. (b) Sharma, J.; Yeh, H.-C.; Yoo, H.; Werner, J. H.; Martinez, J. S. *Chem. Commun.* **2011**, *47*, 2294–2296.
- (34) (a) Guo, W.; Yuan, J.; Dong, Q.; Wang, E. *J. Am. Chem. Soc.* **2010**, *132*, 932–934. (b) Yeh, H.-C.; Sharma, J.; Shih, I.-M.; Vu, D. M.; Martinez, J. S.; Werner, J. H. *J. Am. Chem. Soc.* **2012**, *134*, 11550–11558. (c) Yeh, H.-C.; Sharma, J.; Han, J. J.; Martinez, J. S.; Werner, J. H. *Nano Lett.* **2010**, *10*, 3106–3110. (d) Petty, J. T.; Sengupta, B.; Sotry, S. P.; Degtyareva, N. N. *Anal. Chem.* **2011**, *83*, 5957–5964.
- (35) (a) Liu, Y.-Q.; Zhang, M.; Yin, B.-C.; Ye, B.-C. *Anal. Chem.* **2012**, *84*, 5165–5169. (b) Yang, S. W.; Vosch, T. *Anal. Chem.* **2011**, *83*, 6935–6939. (c) Shah, P.; Rørvig-Lund, A.; Chaabane, S. B.; Thulstrup, P. W.; Kjaergaard, H. G.; Fron, E.; Hofkens, J.; Yang, S. W.; Vosch, T. *ACS Nano* **2012**, *6*, 8803–8814.
- (36) (a) Li, J.; Zhong, X.; Cheng, F.; Zhang, J.-R.; Jiang, L.-P.; Zhu, J.-J. *Anal. Chem.* **2012**, *84*, 4140–4146. (b) Sun, Z.; Wang, Y.; Wei, Y.; Zhu, H.; Cui, Y.; Zhao, Y.; Gao, X. *Chem. Commun.* **2011**, *47*, 11960–11962.
- (37) Katari, J. E. B.; Colvin, V. L.; Alivisatos, A. P. *J. Phys. Chem.* **1994**, *98*, 4109–4117.
- (38) (a) Liu, X.; Shi, L.; Niu, W.; Li, H.; Xu, G. *Biosens. Bioelectron.* **2008**, *23*, 1887–1890. (b) Liu, X.; Niu, W.; Li, H.; Han, S.; Hu, L.; Xu, G. *Electrochem. Commun.* **2008**, *10*, 1250–1253.
- (39) Seo, S.-Y.; Sharma, V. K.; Sharma, N. *J. Agric. Food Chem.* **2003**, *51*, 2837–2853.
- (40) (a) Li, X.; Shi, W.; Chen, S.; Jia, J.; Ma, H.; Wolfbeis, O. S. *Chem. Commun.* **2010**, *46*, 2560–2562. (b) Li, D.; Gill, R.; Freeman, R.; Willner, I. *Chem. Commun.* **2006**, 5027–5029.
- (41) Millan, J. L. *Mammalian Alkaline Phosphatases: From Biology to Applications in Medicine and Biotechnology*; WILEY-VCH Verlag GmbH & Co. KGaA: Weinheim, 2006.
- (42) Mishra, S.; Hamburger, A. W. *Cancer Res.* **1993**, *53*, 557–563.
- (43) Miao, Y.; He, N.; Zhu, J.-J. *Chem. Rev.* **2010**, *110*, 5216–5234.